

Computational verification of large logical models - application to the prediction of T cell response to checkpoint inhibitors

Céline Hernandez^{1,2}, Morgane Thomas-Chollier^{1,3}, Aurélien Naldi^{1,4,*}, Denis Thieffry^{1,*}

¹ *Institut de Biologie de l'ENS (IBENS), Département de biologie, École normale supérieure, CNRS, INSERM, Université PSL, 75005 Paris, France*

² *New address: Institute for Integrative Biology of the Cell (I2BC), CEA, CNRS, Univ. Paris-Sud, Université Paris-Saclay, 91198, Gif-sur-Yvette cedex, France*

³ *Institut Universitaire de France*

⁴ *New address: Lifeware Project, INRIA Paris-Saclay, France*

Correspondence*:

aurelien.naldi@gmail.com, denis.thieffry@bio.ens.psl.eu

2 ABSTRACT

3 At the crossroad between biology and mathematical modelling, computational systems biology
4 can contribute to a mechanistic understanding of high-level biological phenomenon. But as
5 knowledge accumulates, the size and complexity of mathematical models increase, calling for
6 the development of efficient dynamical analysis methods. Here, we propose the use of two
7 approaches for the development and analysis of complex cellular network models.

8 A first approach, called "model verification" and inspired by unitary testing in software
9 development, enables the formalisation and automated verification of validation criteria for whole
10 models or selected sub-parts. When combined with efficient analysis methods, this approach is
11 suitable for continuous testing, thereby greatly facilitating model development.

12 A second approach, called "value propagation", enables efficient analytical computation of
13 the impact of specific environmental or genetic conditions on the dynamical behaviour of some
14 models.

15 We apply these two approaches to the delineation and the analysis of a comprehensive model
16 for T cell activation, taking into account CTLA4 and PD-1 checkpoint inhibitory pathways. While
17 model verification greatly eases the delineation of logical rules complying with a set of dynamical
18 specifications, propagation provides interesting insights into the different potential of CTLA4 and
19 PD-1 immunotherapies.

20 Both methods are implemented and made available in the all-inclusive CoLoMoTo Docker image,
21 while the different steps of the model analysis are fully reported in two companion interactive
22 jupyter notebooks, thereby ensuring the reproduction of our results.

23 **Keywords:** T Cell, checkpoint inhibitors, Boolean models, model verification, value propagation.

1 INTRODUCTION

24 Recent technical developments have allowed scientists to study immunology and health-related issues
25 from a variety of angles. For many diseases, especially for cancer, the current trend consists in aggregating
26 data coming from different sources to gain a global view of cell, tissue, or organ dysfunction. Over the
27 last decades, diverse mathematical frameworks have been proposed to seize a multiplicity of biological
28 questions (Le Novère, 2015), including in immunology (Kaufman et al., 1985, 1999; Eftimie et al., 2016;
29 Chakraborty, 2017). However, the increasing complexity of biological questions implies the development
30 of more sophisticated models, which in turn bring serious computational challenges.

31 Among the mathematical approaches proposed for the modelling of cellular networks, the logical
32 modelling framework is increasingly used. In particular, it has been successfully applied to immunology
33 and cancer, leading to the creation of models encompassing dozens of components, some including many
34 inputs components (Grieco et al., 2013; Abou-Jaoudé et al., 2014; Flobak et al., 2015; Oyeyemi et al.,
35 2015). However, the large size of recent models hinders the complete exploration of their dynamical
36 behaviour through simulation, especially in non-deterministic settings.

37 To address these difficulties, we define and apply a *model verification* approach to systematically verify
38 whether a model complies with a list of known properties (section 2). These properties are defined as
39 model *specifications*, either at a local (i.e. for sub-models) or at a global level. This automated verification
40 procedure fosters confidence during the development of a complex dynamical model and paves the way to
41 the development of models with hundreds of nodes.

42 We further outline and apply a *value propagation* method, which enables the assessment of the impact of
43 environmental or genetic constraints on the dynamical behaviour of complex cellular networks (section 3).

44 These two complementary approaches can be applied to the development and analysis of large dynamical
45 models, as illustrated in Figure 1. Noteworthy, they have been implemented in a multi-platform Docker
46 image combining various complementary logical modelling and analysis tools (Naldi et al., 2018b). We
47 further illustrate the power of these methods through the analysis of an original model described in Section 4.
48 The different steps of analysis are fully reported in two companion interactive jupyter notebooks, available
49 with the model on the GINsim website (<http://ginsim.org/model/tcell-checkpoint-inhibitors-tcla4-pd1>),
50 thereby ensuring their reproducibility.

2 MODEL VERIFICATION

51 2.1 A software engineering framework for logical model building

52 One of the main features determining the interest of a model is its ability to accurately recapitulate salient
53 biological knowledge. More precisely, this knowledge can be used in two complementary ways during
54 the model building process. On the one hand, it is used to define the model architecture, specifying which
55 biological entities need to be included and which interactions between these entities need to be encoded. On
56 the other hand, biological knowledge entails dynamical properties that must be achieved by the resulting
57 model, whether transitory or asymptotic, to account for biological observations. These properties induce
58 satisfaction criteria and must be clearly specified for rigorous model assessment or comparison with other
59 models. Failures to reproduce such properties need to be carefully documented, thereby providing a basis
60 for further model improvement.

61 In the domain of logical modeling applied to cellular networks, various formal methods have already
62 been proposed to verify dynamical properties. For example *stable states* (or textitfixed points, characterised
63 by all components being steady at the same time) tentatively correspond to asymptotic properties that

64 can used to assess the reproduction of known persistent biological behaviour. More complex asymptotic
65 behaviours include *cyclic attractors*, which can be approximate by the computation of so called *trap spaces*.
66 Also called *stable motifs*, trap spaces are hypercubes in the state space such that all successors of all states
67 in the hypercube also belong to it (for synchronous and asynchronous updatings, or any other updating).
68 These hypercubes then provide an approximation of complex attractors. Trap spaces and stable states can
69 be defined as results of a constraint solving system, enabling their efficient computation (Klarner et al.,
70 2018). Their reachability however must be assessed separately, often using model checking or stochastic
71 simulations, which requires longer computations.

72 Model checking techniques have been successfully applied to specify and verify temporal constraints on
73 a model behaviour (Monteiro and Chaouiya, 2012; Miskov-Zivanov et al., 2016; Traynard et al., 2016;
74 Wang et al., 2016).

75 In any case, whatever the formalism chosen, the building of a complex dynamical model is intrinsically
76 iterative, as its establishment is usually incremental and requires continuous testing and adjustment with
77 reference to a growing body of biological knowledge.

78 In the field of software engineering, the similar need to repeatedly assess criteria of success or failure of a
79 software program led to the development of powerful *software verification* techniques, and in particular
80 to software testing (Myers, 1979), which main goal is to assess whether a software meets a series of
81 well-defined requirements. More importantly, such assessments must be repeated as soon as a new piece of
82 code or specification is added. Software testing aims to check whether newly introduced modification might
83 break any of the previous performances. In particular, software verification includes the notion of *unit*
84 *testing*, where suites of tests describe the expected behaviour associated with individual units composing a
85 program. This idea can be transposed from computer science to model building and has been successfully
86 applied in the context of other modeling frameworks (Hoops et al., 2006; Lopez et al., 2013; Sarma et al.,
87 2016; Boutillier et al., 2018), but not yet to logical modeling.

88 Here, we transpose the *unit testing* approach to integrate a comprehensive series of verifiable criteria,
89 from the early stages of model conception, in order to fully automate the dynamical evaluation of logical
90 models. The core idea is to split the biological knowledge on which a model is based into individual
91 verifiable criteria that can be formalised as specifications (Figures 1 and 2). In this respect, individual units
92 of knowledge, derived from the scientific literature or biological experiments, must be formulated into
93 stable or dynamical properties. Each specification, coupling a property with an expected value, can serve
94 as a basis to define a test case for a model. Testing such a specification amounts to compute an "observed"
95 value based on the model and compare this value to the expected one.

96 In practice, the CoLoMoTo notebook environment (Naldi et al., 2018b) provides a Python API for
97 several software tools, enabling the definition of a wide range of dynamical analysis for the computation of
98 observed values. Individual test cases can be assembled into a library, also called *testing suite*. Existing
99 tools and packages enabling software testing can then be applied to automatically assess whether a model
100 satisfies (or not) a series of specifications. In this study, we used the python package 'unittest', taking
101 advantage of its seamless integration into the CoLoMoTo interactive notebook. This unit-testing package is
102 integrated by default into the recent versions of the Python standard library (<http://python.org>).

103 **2.2 Local verification of sub-models can cope with sparsity of biological knowledge**

104 Biological knowledge reported in the scientific literature is often insufficient to evaluate a comprehensive
105 model, which may encompass hundreds of nodes. In particular, observations regarding component activity

106 often relate to only a limited subset of nodes of the model. This greatly complicates the definition of
107 specifications for the whole model.

108 Given a comprehensive model and a set of components of interest, one can extract a sub-model containing
109 these core components, along with their associated logical rules. Components which take part of these
110 logical rules but are not part of the selected set are considered as external inputs of the sub-model (Figure 2).
111 This functionality has been implemented in the 'submodel' function of the Java bioLQM library (Naldi,
112 2018) according to the following procedure.

113 Let $M = (V, f)$ be a model, where V is the set of components, and f the update function. For each
114 c in V , f_c is the logical function associated to the component c and $R(c)$ is the set of its regulators (i.e.
115 components that intervene in the logical rule). Given a list of selected components $C \subset V$:

- 116 1. $S = \emptyset$
- 117 2. for each component $c \in C$: $S = S + \{c\} + R(c)$
- 118 3. create the sub-model $M' = (S, f')$ such that for each component c in S : $f'_c = \begin{cases} f_c & \text{if } R(c) \subset S \\ c & \text{otherwise} \end{cases}$

119 As shown in Section 4, the delineation of such sub-models can greatly facilitate the definition and
120 verification of local specifications.

3 VALUE PROPAGATION ENABLES THE EVALUATION OF THE IMPACT OF A GIVEN CELLULAR ENVIRONMENT ON MODEL DYNAMICS

121 The core idea of *value propagation* is presented in Figure 3. Given a set of logical rules and a cellular
122 context, an iterative algorithm enables the computation of the dynamical consequences of the cellular
123 context on all the components of the model.

124 First, the cellular context is formalised by assigning constant values to some components of the model.
125 Next, we apply a recent model reduction technique reported by Saadatpour *et al.* (Saadatpour et al., 2013).
126 Briefly, for each constant node, the corresponding value is inserted into the logical rule associated with
127 each of its target nodes. Each logical rule is then simplified using Boolean algebra. If the rule simplifies to
128 a constant, this fixed value is further propagated into the logical rules of downstream nodes. This process is
129 iterated until no further propagation or simplification can be made on the logical rules of the model. In
130 contrast with the approach of Saadatpour *et al.*, which aims at producing a reduced model, we focus
131 principally on the outcome of the propagation of fixed values.

132 The result of value propagation can be very informative by itself. Indeed, the resulting stabilised values
133 provide insights into the impact of a given (single or multiple) perturbation on the model, revealing which
134 elements are consequently constrained to become activated or inactivated, versus which elements keep
135 some degree of freedom. Furthermore, this method greatly eases the comparison of the impacts of different
136 biological contexts on network dynamics by performing a differential analysis of the corresponding lists
137 and target values of fixed components. This method has multiple advantages when applied to complex
138 networks, as it can be used efficiently on models with large numbers of components. It further simplifies
139 the computation of attractors (stable states or even simple or complex cycles). Interestingly, Saadatpour
140 and collaborators showed that this method conserves the stable states and complex attractors under the
141 fully asynchronous updating assumption (Saadatpour et al., 2013).

142 This method was extended to multilevel models and implemented into the Java bioLQM library (Naldi,
143 2018). In this implementation, the fixed components are conserved during value propagation, enabling a
144 direct comparison of the propagated effects of alternative perturbations.

145 The power of this approach is demonstrated on a concrete example in the following section.

4 APPLICATION: ASSESSING THE EFFECT OF CHECKPOINT BLOCKADE THERAPIES ON T CELL ACTIVATION

146 4.1 Biological background

147 Over the last decades, immunotherapies have been the subject of intense studies and led to great advances
148 in the field of cancer treatment. Through the years, it has then been recognised that T cells often display
149 a reduced ability to eliminate cancer cells, and that expression of co-inhibitory receptors at their surface
150 accounts for this compromised function. Receptors like Cytotoxic T-lymphocyte protein 4 (CTLA4, also
151 known as CD152) (Walunas et al., 1994; Leach et al., 1996) and Programmed cell death protein 1 (PD-1,
152 also known as PDCD1 or CD279) (Ishida et al., 1992) have been particularly studied in that context.
153 Antibodies blocking the pathways downstream of these co-inhibitors (checkpoint blockade therapies) have
154 become standard treatment for metastatic melanoma (Robert et al., 2011; Simpson et al., 2013) and other
155 cancers (Ribas and Wolchok, 2018), including non-small cell lung cancer, renal cell carcinoma, Hodgkin's
156 lymphoma, Merkel cell carcinoma and many others. The successes of these studies led to an increasing
157 interest in T cell co-inhibitory receptors.

158 Nevertheless, a clear understanding of the mechanisms at work inside T cells remains elusive. Therapies
159 targeting CTLA4 or PD-1 show different immune adverse effects (June et al., 2017), while the corresponding
160 intra-cellular mechanisms remain to be clarified. Moreover, a rationale for the educated development of
161 new immunotherapies focusing on other receptors or combinations of receptors is clearly needed. Co-
162 inhibitory receptors are legions at the surface of T cells (Brownlie and Zamoyska, 2013) and biology of
163 T cell activation or tolerance involves activation or repression of highly interconnected and complicated
164 pathways (Baumeister et al., 2016).

165 Given the central role of T cells in many medical contexts, several mathematical frameworks have
166 been applied to model T cell activation. Recent examples include rule-based approaches (Chylek et al.,
167 2014), ordinary differential equations (Perley et al., 2014), and logical models (Oyeyemi et al., 2015;
168 Rodríguez-Jorge et al., 2019; Sánchez-Villanueva et al., 2019), considering different biomedical contexts
169 as diverse as HIV infection or neonate vaccination. To our knowledge, none of them specifically focused
170 on the impact of co-inhibitory receptors on T cell activation or tolerance.

171 In this study, we applied the logical framework to integrate current data on CTLA4 and PD-1 pathways
172 and assess their impact on T cell activation. Our goal was triple. First, we wanted to create a comprehensive
173 model building upon extensive knowledge encoded into a molecular map (see next section). Second, using
174 model verification and a specific unit test suite, we aimed to firmly anchor the model at both the global and
175 local scale into the collected biological knowledge. Third, using value propagation, we aimed to provide a
176 tool for the comparative analysis of intra-cellular consequences when targeting CTLA4 versus PD-1 T-cell
177 co-receptors.

178 4.2 Comprehensive molecular mapping of T Cell activation network

179 Prior to mathematical modelling, knowledge about biological entities involved in T Cell activation was
180 collected from available pathway databases, including Reactome (Fabregat et al., 2016), PantherDB (Mi

181 et al., 2013), ACSN (Kuperstein et al., 2015) and WikiPathways (Slenter et al., 2018). Moreover, the
182 scientific literature indexed in the PubMed database was further explored and carefully curated. Using
183 the software CellDesigner (version 4.3.1) (Funahashi et al., 2008), this knowledge was encoded in a
184 molecular map describing reactions between biological entities (either proteins, RNAs, genes, complexes or
185 metabolites). Each biological entity included in the map was annotated with a series of standard identifiers,
186 including UniProtKB accession number, recommended and alternative names, gene name and synonyms,
187 and cross-references to unique HGNC identifiers and approved symbols. The annotations also reference
188 relevant scientific articles, including PubMed identifier, first and last authors, year of publication, and a list
189 of observations extracted from these publications.

190 Our T cell activation map currently encompasses 726 biological entities, in different states (active/inactive,
191 with or without post-translational modifications), and 539 reactions involving these entities (Supplementary
192 Figure 1 and File 1). Globally, the map currently integrates information from 123 scientific articles, which
193 are cited in the annotations of the entities and reactions of the map.

194 **4.3 Logical modelling of T Cell activation**

195 Using the logical modelling software *GINSim* (version 3.0.0b) (Naldi et al., 2018a), we then manually
196 derived a regulatory graph encompassing 216 nodes and 451 arcs (Figure 4) from the content of the
197 molecular map. One by one, biological entities represented in the molecular map were re-created as
198 components of the logical model. In most of the cases, the representation of entities having different states
199 was further compressed into a single component summarizing their activity in the TCR signalling cascade.
200 Furthermore, to obtain a dynamical logical model, a specific logical rule must be assigned to each node.
201 In many cases, this can be achieved rather easily based on published data. For more complex situations,
202 a default generic logical rule was initially considered, where all activators are needed for the activation
203 of a component (using the AND operator) and where only one inhibitor is sufficient to repress it (using
204 the OR and NOT operators), which served as a basis for further rule refinement. In some cases, however,
205 in particular when a component is the target of various regulatory interactions or when metabolites are
206 involved, finding direct support for a specific rule may be tricky or impossible. Hence, the delineation of
207 consistent logical rules for a complex model is often the result of an iterative process, starting with generic
208 rules and progressively correcting them based on the results of various analyses.

209 Hereafter, we demonstrate how we can take advantage of the methods presented in the previous sections to
210 ease rule refinement by model verification. We first defined a series of properties expected for the model (see
211 examples in Table 1). Next, stable states and/or trap spaces were computed and automatically compared with
212 these properties (cf. first Jupyter notebook provided on the model web page at <http://ginsim.org/model/tcell-checkpoint-inhibitors-tcla4-pd1>). After some iterative runs of the notebook, manual refinements lead us to
214 a set of rules complying with all the tests.

215 For example, the Endoplasmic Reticulum (ER) serves as a reservoir for calcium ions. This reservoir can be
216 emptied through activation of the Inositol 1,4,5-trisphosphate receptor (IP3R1). When empty, this reservoir
217 can be filled through activation of the Sarcoplasmic/endoplasmic reticulum calcium ATPase 2 (SERCA)
218 pumps. A default logical rule for a node representing the presence of this Calcium quantity (Calcium_ER)
219 is then 'SERCA AND NOT IP3R1'. To check the behaviour of the corresponding logical sub-model, we
220 defined a test checking whether whenever Calcium_ER was evaluated to TRUE, SERCA was evaluated
221 to FALSE (see test 'test_calc_tp_rest_ER1_SERCA0'). However, consecutive model verification failed,
222 allowing us to notice that the default rule implied that SERCA should be always TRUE for Calcium_ER to

223 be TRUE. The rule was then corrected to take into account the fact that Calcium_ER should stay TRUE
224 whenever it would reach this value in absence of IP3R1.

225 In the first Jupyter notebook provided as supplementary material, we include all the code enabling the
226 verification of our final model, which encompasses 36 unit tests split in four test suites. On a MacBook Pro
227 using macOS 10.13 High Sierra, with a 2.3 GHz Intel Core i7 and 16GB 1600 MHz DDR3, all the tests
228 were run in 87s.

229 The four test suites cover the most complex parts of the model, some of them particularly difficult to
230 define. These suites use sub-models, whose delineation was guided by known pathways and practical
231 knowledge gained by the modeler during the assembly of the molecular map. The Calcium module test
232 suite covers a sub-model related to the fluxes of Calcium ions between different cellular compartments,
233 namely the endoplasmic reticulum, the cytoplasm and the extracellular region. The LCK module test
234 suite is centered on the Tyrosine-protein kinase Lck (LCK). This kinase is known to have multiple sites
235 of phosphorylation, whose collective status determines the tridimensional conformation and thus the
236 activity of the enzyme (Ventimiglia and Alonso, 2013). The Cytoskeleton module test suite covers the
237 cytoskeleton remodelling events occurring during T cell activation, and has strong connections with the
238 Calcium sub-model. Finally, the Anergy/activation/differentiation module covers a less documented module
239 encompassing the nucleus compartment and gene transcription.

240 **4.4 Comparison of the impacts of CTLA4 and PD-1 co-inhibitory receptors through** 241 **value percolation**

242 Based on the model described in the preceding section, a comparative propagation analysis was performed
243 to visualise the respective effects of CTLA4 and PD-1 receptor activation on model dynamics. Figure 5
244 displays the value propagation for each condition on a single regulatory graph, using a color code to
245 distinguish the different situations (component inhibition/activation in one or both conditions). The value
246 propagation for the two conditions are further shown separately in the second companion notebook
247 (available at <http://ginsim.org/model/tcell-checkpoint-inhibitors-tcla4-pd1>). This analysis reveals that
248 the activation of the CTLA4 receptor impacts most pathways of the model, impeding in particular the
249 remodeling of the cytoskeleton and the metabolic switch associated with bona fide T cell activation. In
250 contrast, the activation of the PD-1 receptor leads to more limited effects, predominantly freezing the
251 components of the NF- κ B pathway.

252 A more refined comparative analysis of value propagation from these two receptor activations entails the
253 observation that the set of nodes frozen by the propagation of PD-1 activation is completely included inside
254 the set of nodes frozen by the propagation of CTLA4 activation (see Table 2). Furthermore, the values of
255 the components frozen in both propagation studies are the same. Interestingly, a set of nodes related to
256 calcium influx from and to the endoplasmic reticulum remain unfixed by any of the propagation analyses.
257 This could be an artefact of the positive feedback loops added on the nodes representing the Calcium ion
258 levels in different compartments and would need to be further investigated. A more detailed biological
259 interpretation of these results is proposed in the following section.

260 **5 CONCLUSIONS AND PROSPECTS**

260 In this study, we have implemented and applied two complementary methods enabling a specification-
261 oriented model building approach, thereby easing the delineation and analysis of highly complex logical
262 models. In this respect, the building of a knowledge base, e.g. in terms of a molecular map, is an important

263 first step. In the molecular map (provided as the supplementary File 1), we have integrated the most relevant
264 biological references available on T cell activation and inhibition pathways.

265 This map is clearly due to evolve, in particular thanks to the generation and analysis of novel high-
266 throughput data (see e.g. the recent extensive analysis of the TCR signalosome (Voisinne et al., 2019)). But
267 any modification needs to be manually propagated to the dynamical model. To date, methods to derive
268 proper dynamical models from such molecular maps are still in their infancy. In the particular case of the
269 Boolean framework, only one automated approach has been recently proposed (Aghamiri et al., 2020).
270 However, a limitation of this approach is the generation of generic logical rules based on static knowledge.
271 Hence, the methods presented here could be used to advantageously refine these rules, taking into account
272 additional biological knowledge about the behaviour of the system under study.

273 We used the information gathered in our T cell activation map to build a dynamical logical model
274 encompassing over 200 components and 450 interactions. For such a complex model, defining the
275 logical rules in concordance with biological knowledge is a difficult and error-prone process, usually
276 involving iterative trial simulations, where failures are identified to suggest potential improvements. Hence,
277 listing comprehensive and consistent model specifications is a crucial step for model construction. These
278 specifications can be revised as the modeller deepens his understanding of the biological processes under
279 study. Noteworthy, such systematic testing procures a sense of confidence during the development process.

280 In the unit tests developed for our model, the definition of sub-models was guided by biological knowledge
281 and pathway definitions, while relying partly on the modeller intuition. This step could be improved by
282 community analyses of the regulatory graph to improve their definition.

283 Model checking techniques have been previously applied to assess model behaviour through systematic
284 cycles of model refinements (see e.g. Traynard et al. (2016) and reference therein). Model verification, as
285 defined here, is a generalisation of this approach, as it can rely on any available analysis as long as its result
286 can be compared to an expected outcome. In our hands, in the course of model building, the unit testing
287 approach, strongly anchored to available knowledge, proved to be very efficient to assess and improve
288 model consistency with respect to a list of biological specifications, without the need of time-consuming
289 and costly simulations. Implemented in the CoLoMoTo Interactive notebook framework (Naldi et al.,
290 2018b), this approach enabled us to define a model recapitulating the most salient properties observed in
291 response to T cell activation, including quiescence, anergy and differentiation.

292 The use of model checking techniques could be further extended to assess the sensitivity of model
293 behaviour to the choice of specific logical rules. Such extension is hindered by the exponential increase of
294 the number of possible logical rule, as the number of regulators increases. We would thus need a rationale
295 to explore the space of logical rules. A first step in this direction can be found in Abou-Jaoudé and Monteiro
296 (2019).

297 The approach presented here could also be improved by taking into account and tracking uncertainty
298 during model conception (Thobe et al., 2018), or yet by taking advantage of computational repairing
299 methods (Gebser et al., 2010) to identify more precisely remaining inconsistencies with biological data.
300 Furthermore, other software engineering techniques, such as *code coverage*, could be borrowed to further
301 improve model building and verification. As code coverage computes how much of a program's code is
302 covered by unit tests, one could design a method computing the fraction of the components of a model that
303 is effectively covered by specifications.

304 Value propagation analysis of our large and complex regulatory graph proved to be biologically insightful.
305 Indeed, this straightforward approach enabled us to clearly contrast the respective impacts of CTLA4 and

306 PD-1 on T cell activation in our model, providing some rationale for their differential effects in current
307 therapeutic studies. Indeed, anti-CTLA4 immunotherapies are known for their strong adverse effects related
308 to autoimmunity and immunotoxicity (June et al., 2017). Anti-CTLA4 immunotherapies are currently
309 combined with anti-PD-1 immunotherapy, known for its milder impact on the immune system.

310 Interestingly, the state of the node representing the Interleukin 2 (IL2) cytokine activation illustrates the
311 differences of action of these receptors. Activation of the IL2 gene depends mainly on the activation of
312 three transcription factors: the Nuclear Factor of Activated T cells (NFAT), the AP1 complex, and the
313 Nuclear factor NF-kappa-B (NF- κ B) (Smith-Garvin et al., 2009). When NFAT and AP1 are both active,
314 they form a complex and together bind a regulatory region of the IL2 gene. In absence of AP1, NFAT
315 induces a different program leading to cellular anergy (Macian, 2005; Smith-Garvin et al., 2009): activation
316 of Diacylglycerol Kinase (DGK) prevents DAG-mediated activation of RasGRP1, which regulates the
317 threshold for T cell activation (Roose et al., 2007; Das et al., 2009).

318 Our comparative propagation analysis reveals that while the activation of the CTLA4 receptor leads
319 to a general inactivation of the three transcription factors regulating IL2 production, activation of the
320 PD-1 receptor leads only to the inactivation of NF- κ B and FOS (a member of the AP1 complex), thereby
321 preventing the formation of the NFAT/AP1 complex, but enabling the activation of DGK. This observation is
322 consistent with the proposal to target DGK isoforms as a complement of checkpoint immunotherapy (Riese
323 et al., 2016; Jung et al., 2018).

324 As a next step, new co-inhibitory receptors recently under study, such as the Hepatitis A virus cellular
325 receptor 2 (also known as TIM3) or the Lymphocyte activation gene 3 protein (LAG-3) (Anderson et al.,
326 2016), could be easily added to the model described here, provided sufficient information could be
327 gathered regarding their interacting partners. Applying propagation analysis in this context would be
328 greatly insightful for future therapy developments.

CONFLICT OF INTEREST STATEMENT

329 The authors declare that the research was conducted in the absence of any commercial or financial
330 relationships that could be construed as a potential conflict of interest.

AUTHOR CONTRIBUTIONS

331 CH developed the T cell signalling molecular map and model under the supervision of MTC and DT.
332 CH and AN implemented the computational methods and applied them to the T cell model under the
333 supervision of AN and DT. All co-authors contributed to the redaction of the manuscript and endorse its
334 content.

FUNDING

335 This work was supported by a grant from the French Plan Cancer (project SYSTAIM, 2015–2019).

ACKNOWLEDGMENTS

336 We warmly thank Bernard Malissen, Romain Roncagalli and Guillaume Voisinne, for their thoughtful
337 guidance during the construction of the T cell signalling model.

SUPPLEMENTAL DATA

338 Supplementary Figure 1: Molecular map in good resolution or vectorial format
339 map describes biological entities and reactions implicated in the process leading to activation of CD4+ T

340 cells in humans/mouse. The cytoplasmic membrane and attached receptor proteins are placed at the top,
341 while the cell nucleus is located at the bottom. Reactions represent current knowledge of various pathways
342 related to cytoskeletal remodelling, calcium fluxes, metabolism, cell cycle or IL2 production, and are
343 encoded using the CellDesigner software (Funahashi et al., 2008) (the CellDesigner file is provided as
344 Supplementary File 1).

345 Supplementary File 1: Molecular map in CellDesigner/XML format (Funahashi et al., 2008).

DATA AVAILABILITY STATEMENT

346 In addition, the original model (GINsim format - zginml) can be downloaded from the GINsim
347 website (<http://ginsim.org/model/tcell-checkpoint-inhibitors-tcla4-pd1>), together with previews of the two
348 interactive notebooks enabling the reproduction of all the analyses and results reported in this study, using
349 the tools integrated in the most recent CoLoMoTo Docker image (<https://github.com/colomoto/colomoto-docker>). A SBML-qual export of the logical model is also available on the GINsim model repository page,
350 which will be further deposited into the database BioModels (<https://www.ebi.ac.uk/biomodels/>) upon
351 publication.
352

REFERENCES

- 353 Abou-Jaoudé, W. and Monteiro, P. T. (2019). On logical bifurcation diagrams. *Journal of Theoretical*
354 *Biology* 466, 39–63. doi:10.1016/j.jtbi.2019.01.008
- 355 Abou-Jaoudé, W., Monteiro, P. T., Naldi, A., Grandclaudon, M., Soumelis, V., Chaouiya, C., et al. (2014).
356 Model checking to assess T-helper cell plasticity. *Frontiers in bioengineering and biotechnology* 2, 86.
357 doi:10.3389/fbioe.2014.00086
- 358 Aghamiri, S. S., Singh, V., Naldi, A., Helikar, T., Soliman, S., and Niarakis, A. (2020). Automated
359 inference of Boolean models from molecular interaction maps using CaSQ. *Bioinformatics* , 1–13doi:10.
360 1093/bioinformatics/btaa484
- 361 Anderson, A. C., Joller, N., and Kuchroo, V. K. (2016). Lag-3, Tim-3, and TIGIT: Co-inhibitory Receptors
362 with Specialized Functions in Immune Regulation. *Immunity* 44, 989–1004. doi:10.1016/j.immuni.2016.
363 05.001
- 364 Baumeister, S. H., Freeman, G. J., Dranoff, G., and Sharpe, A. H. (2016). Coinhibitory Pathways
365 in Immunotherapy for Cancer. *Annual Review of Immunology* 34, 539–573. doi:10.1146/
366 annurev-immunol-032414-112049
- 367 Boutillier, P., Maasha, M., Li, X., Medina-Abarca, H. F., Krivine, J., Feret, J., et al. (2018). The Kappa
368 platform for rule-based modeling. *Bioinformatics (Oxford, England)* 34, i583–i592. doi:10.1093/
369 bioinformatics/bty272
- 370 Brownlie, R. J. and Zamoyska, R. (2013). T cell receptor signalling networks: branched, diversified and
371 bounded. *Nature reviews. Immunology* 13, 257–69. doi:10.1038/nri3403
- 372 Chakraborty, A. K. (2017). A Perspective on the Role of Computational Models in Immunology. *Annual*
373 *review of immunology* 35, 403–439. doi:10.1146/annurev-immunol-041015-055325
- 374 Chylek, L. A., Akimov, V., Dengjel, J., Rigbolt, K. T. G., Hu, B., Hlavacek, W. S., et al. (2014).
375 Phosphorylation site dynamics of early T-cell receptor signaling. *PloS one* 9, e104240. doi:10.1371/
376 journal.pone.0104240
- 377 Das, J., Ho, M., Zikherman, J., Govern, C., Yang, M., Weiss, A., et al. (2009). Digital Signaling and
378 Hysteresis Characterize Ras Activation in Lymphoid Cells. *Cell* 136, 337–351. doi:10.1016/j.cell.2008.
379 11.051

- 380 Eftimie, R., Gillard, J. J., and Cantrell, D. A. (2016). Mathematical Models for Immunology: Current
381 State of the Art and Future Research Directions. *Bulletin of Mathematical Biology* 78, 2091–2134.
382 doi:10.1007/s11538-016-0214-9
- 383 Fabregat, A., Sidiropoulos, K., Garapati, P., Gillespie, M., Hausmann, K., Haw, R., et al. (2016). The
384 reactome pathway knowledgebase. *Nucleic Acids Research* 44, D481–D487. doi:10.1093/nar/gkv1351
- 385 Flobak, Å., Baudot, A., Remy, E., Thommesen, L., Thieffry, D., Kuiper, M., et al. (2015). Discovery of
386 Drug Synergies in Gastric Cancer Cells Predicted by Logical Modeling. *PLoS computational biology* 11,
387 1–20. doi:10.1371/journal.pcbi.1004426
- 388 Funahashi, B. A., Matsuoka, Y., Jouraku, A., Morohashi, M., Kikuchi, N., and Kitano, H. (2008).
389 A Versatile Modeling Tool for Biochemical Networks. *Proceedings of the IEEE* 96, 1254–1265.
390 doi:10.1109/JPROC.2008.925458
- 391 Gebser, M., Guziolowski, C., Ivanchev, M., Schaub, T., Siegel, A., Veber, P., et al. (2010). Repair and
392 Prediction (under Inconsistency) in Large Biological Networks with Answer Set Programming. In
393 *Principles of Knowledge Representation and Reasoning* (Toronto, Canada: AAAI Press), Principles of
394 Knowledge Representation and Reasoning: Proceedings of the Twelfth International Conference, KR
395 2010
- 396 Grieco, L., Calzone, L., Bernard-Pierrot, I., Radvanyi, F., Kahn-Perlès, B., and Thieffry, D. (2013).
397 Integrative modelling of the influence of MAPK network on cancer cell fate decision. *PLoS*
398 *computational biology* 9, e1003286. doi:10.1371/journal.pcbi.1003286
- 399 Hoops, S., Gauges, R., Lee, C., Pahle, J., Simus, N., Singhal, M., et al. (2006). COPASI - A COMplex
400 PATHway SIMulator. *Bioinformatics* 22, 3067–3074. doi:10.1093/bioinformatics/btl485
- 401 Ishida, Y., Agata, Y., Shibahara, K., and Honjo, T. (1992). Induced expression of PD-1, a novel member of
402 the immunoglobulin gene superfamily, upon programmed cell death. *The EMBO journal* 11, 3887–95
- 403 June, C. H., Warshauer, J. T., and Bluestone, J. A. (2017). Is autoimmunity the Achilles' heel of cancer
404 immunotherapy? *Nature Medicine* 23, 540–547. doi:10.1038/nm.4321
- 405 Jung, I. Y., Kim, Y. Y., Yu, H. S., Lee, M., Kim, S., and Lee, J. (2018). CRISPR/Cas9-Mediated
406 Knockout of DGK Improves Antitumor Activities of Human T Cells. *Cancer Research* 78, 4692–4703.
407 doi:10.1158/0008-5472
- 408 Kaufman, M., Andris, F., and Leo, O. (1999). A logical analysis of T cell activation and anergy. *Proceedings*
409 *of the National Academy of Sciences of the United States of America* 96, 3894–9
- 410 Kaufman, M., Urbain, J., and Thomas, R. (1985). Towards a logical analysis of the immune response.
411 *Journal of theoretical biology* 114, 527–61
- 412 Klarner, H., Siebert, H., Nee, S., and Heintz, F. (2018). Basins of Attraction, Commitment Sets
413 and Phenotypes of Boolean Networks. *IEEE/ACM Transactions on Computational Biology and*
414 *Bioinformatics* 17, 1115–1124. doi:10.1109/TCBB.2018.2879097
- 415 Kuperstein, I., Bonnet, E., Nguyen, H.-A., Cohen, D., Viara, E., Grieco, L., et al. (2015). Atlas of Cancer
416 Signalling Network: a systems biology resource for integrative analysis of cancer data with Google
417 Maps. *Oncogenesis* 4, e160. doi:10.1038/oncsis.2015.19
- 418 Le Novère, N. (2015). Quantitative and logic modelling of molecular and gene networks. *Nature reviews.*
419 *Genetics* 16, 146–58. doi:10.1038/nrg3885
- 420 Leach, D. R., Krummel, M. F., and Allison, J. P. (1996). Enhancement of antitumor immunity by CTLA-4
421 blockade. *Science* 271, 1734–6. doi:10.1126/science.271.5256.1734
- 422 Lopez, C. F., Muhlich, J. L., Bachman, J. A., and Sorger, P. K. (2013). Programming biological models in
423 Python using PySB. *Molecular Systems Biology* 9, 1–19. doi:10.1038/msb.2013.1

- 424 Macian, F. (2005). NFAT proteins: key regulators of T-cell development and function. *Nature reviews.*
425 *Immunology* 5, 472–84. doi:10.1038/nri1632
- 426 Mi, H., Muruganujan, A., and Thomas, P. D. (2013). PANTHER in 2013: Modeling the evolution of gene
427 function, and other gene attributes, in the context of phylogenetic trees. *Nucleic Acids Research* 41,
428 377–386. doi:10.1093/nar/gks1118
- 429 Miskov-Zivanov, N., Zuliani, P., Wang, Q., Clarke, E. M., and Faeder, J. R. (2016). High-level modeling
430 and verification of cellular signaling. *2016 IEEE International High Level Design Validation and Test*
431 *Workshop, HLDVT 2016*, 162–169doi:10.1109/HLDVT.2016.7748271
- 432 Monteiro, P. T. and Chaouiya, C. (2012). Efficient Verification for Logical Models of Regulatory Networks.
433 In *6th International Conference on Practical Applications of Computational Biology & Bioinformatics*,
434 vol. 6. 259–267. doi:10.1007/978-3-642-28839-5_30
- 435 Myers, G. J. (1979). *The Art of Software Testing* (Wiley Publishing), 1st edn.
- 436 Naldi, A. (2018). BioLQM: A Java Toolkit for the Manipulation and Conversion of Logical Qualitative
437 Models of Biological Networks. *Frontiers in physiology* 9, 1605. doi:10.3389/fphys.2018.01605
- 438 Naldi, A., Hernandez, C., Abou-Jaoudé, W., Monteiro, P. T., Chaouiya, C., and Thieffry, D. (2018a).
439 Logical Modeling and Analysis of Cellular Regulatory Networks With GINsim 3.0. *Frontiers in*
440 *physiology* 9, 646. doi:10.3389/fphys.2018.00646
- 441 Naldi, A., Hernandez, C., Levy, N., Stoll, G., Monteiro, P. T., Chaouiya, C., et al. (2018b). The CoLoMoTo
442 Interactive Notebook: Accessible and Reproducible Computational Analyses for Qualitative Biological
443 Networks. *Frontiers in physiology* 9, 680. doi:10.3389/fphys.2018.00680
- 444 Oyeyemi, O. J., Davies, O., Robertson, D. L., and Schwartz, J. M. (2015). A logical model of HIV-1
445 interactions with the T-cell activation signalling pathway. *Bioinformatics* 31, 1075–1083. doi:10.1093/
446 bioinformatics/btu787
- 447 Perley, J., Mikolajczak, J., Buzzard, G., Harrison, M., and Rundell, A. (2014). Resolving Early Signaling
448 Events in T-Cell Activation Leading to IL-2 and FOXP3 Transcription. *Processes* 2, 867–900. doi:10.
449 3390/pr2040867
- 450 Ribas, A. and Wolchok, J. D. (2018). Cancer immunotherapy using checkpoint blockade. *Science* 359,
451 1350–1355. doi:10.1126/science.aar4060
- 452 Riese, M. J., Moon, E. K., Johnson, B. D., and Albelda, S. M. (2016). Diacylglycerol kinases (DGKs):
453 Novel targets for improving T cell activity in cancer. *Frontiers in Cell and Developmental Biology* 4,
454 1–7. doi:10.3389/fcell.2016.00108
- 455 Robert, C., Miller, W. H., Francis, S., Chen, T.-T., Ibrahim, R., Hoos, A., et al. (2011). Ipilimumab plus
456 Dacarbazine for Previously Untreated Metastatic Melanoma. *New England Journal of Medicine* 364,
457 2517–2526. doi:10.1056/nejmoa1104621
- 458 Rodríguez-Jorge, O., Kempis-Calanis, L., Abou-Jaoudé, W., D.Y., G.-R., Hernandez, C., Ramirez-Pliego,
459 O., et al. (2019). Cooperation between T cell receptor and Toll-like receptor 5 signaling for CD4+ T cell
460 activation. *Science Signaling* 12, eaar3641. doi:10.1126/scisignal.aar3641
- 461 Roose, J. P., Mollenauer, M., Ho, M., Kurosaki, T., and Weiss, A. (2007). Unusual Interplay of Two Types
462 of Ras Activators, RasGRP and SOS, Establishes Sensitive and Robust Ras Activation in Lymphocytes.
463 *Molecular and Cellular Biology* 27, 2732–2745. doi:10.1128/MCB.01882-06
- 464 Saadatpour, A., Albert, R., and Reluga, T. C. (2013). A Reduction Method for Boolean Network
465 Models Proven to Conserve Attractors. *SIAM Journal on Applied Dynamical Systems* 12, 1997–2011.
466 doi:10.1137/13090537x
- 467 Sarma, G. P., Jacobs, T. W., Watts, M. D., Vahid Ghayoomie, S., Larson, S. D., and Gerkin, R. C. (2016).
468 Unit testing, model validation, and biological simulation [version 1; referees: 2 approved, 1 approved

- 469 with reservations]. *F1000Research* 5, 1–17. doi:10.12688/F1000RESEARCH.9315.1
- 470 Simpson, T. R., Li, F., Montalvo-Ortiz, W., Sepulveda, M. A., Bergerhoff, K., Arce, F., et al. (2013).
471 Fc-dependent depletion of tumor-infiltrating regulatory T cells co-defines the efficacy of anti-CTLA-4
472 therapy against melanoma. *The Journal of experimental medicine* 210, 1695–710. doi:10.1084/jem.
473 20130579
- 474 Slenter, D. N., Kutmon, M., Hanspers, K., Riutta, A., Windsor, J., Nunes, N., et al. (2018). WikiPathways:
475 a multifaceted pathway database bridging metabolomics to other omics research. *Nucleic acids research*
476 46, D661–D667. doi:10.1093/nar/gkx1064
- 477 Smith-Garvin, J. E., Koretzky, G. A., and Jordan, M. S. (2009). T Cell Activation. *Annual Review of*
478 *Immunology* 27, 591–619. doi:10.1146/annurev.immunol.021908.132706
- 479 Sánchez-Villanueva, J., Rodríguez-Jorge, O., Ramírez-Pliego, O., Rosas-Salgado, G., Abou-Jaoudé, W., C.,
480 H., et al. (2019). Contribution of ROS and metabolic status to neonatal and adult CD8+T cell activation.
481 *PLoS One* 14, e0226388. doi:10.1371/journal.pone.0226388
- 482 Thobe, K., Kuznia, C., Sers, C., and Siebert, H. (2018). Evaluating uncertainty in signaling networks using
483 logical modeling. *Frontiers in Physiology* 9, 1–15. doi:10.3389/fphys.2018.01335
- 484 Traynard, P., Fauré, A., Fages, F., and Thieffry, D. (2016). Logical model specification aided by model-
485 checking techniques: application to the mammalian cell cycle regulation. *Bioinformatics (Oxford,*
486 *England)* 32, i772–i780. doi:10.1093/bioinformatics/btw457
- 487 Ventimiglia, L. N. and Alonso, M. a. (2013). The role of membrane rafts in Lck transport, regulation and
488 signalling in T-cells. *The Biochemical journal* 454, 169–79. doi:10.1042/BJ20130468
- 489 Voisinne, G., Kersse, K., Chaoui, K., Lu, L., Chaix, J., Zhang, L., et al. (2019). Quantitative interactomics
490 in primary T cells unveils TCR signal diversification extent and dynamics. *Nature Immunology* 20,
491 1530–1541. doi:10.1038/s41590-019-0489-8
- 492 Walunas, T. L., Lenschow, D. J., Bakker, C. Y., Linsley, P. S., Freeman, G. J., Green, J. M., et al.
493 (1994). CTLA-4 can function as a negative regulator of T cell activation. *Immunity* 1, 405–13.
494 doi:10.1016/1074-7613(94)90071-x
- 495 Wang, Q., Miskov-Zivanov, N., Liu, B., Faeder, J. R., Lotze, M., and Clarke, E. M. (2016). Formal
496 Modeling and Analysis of Pancreatic Cancer Microenvironment. In *Computational Methods in Systems*
497 *Biology*, eds. E. Bartocci, P. Lio, and N. Paoletti (Springer International Publishing), 289–305

FIGURES

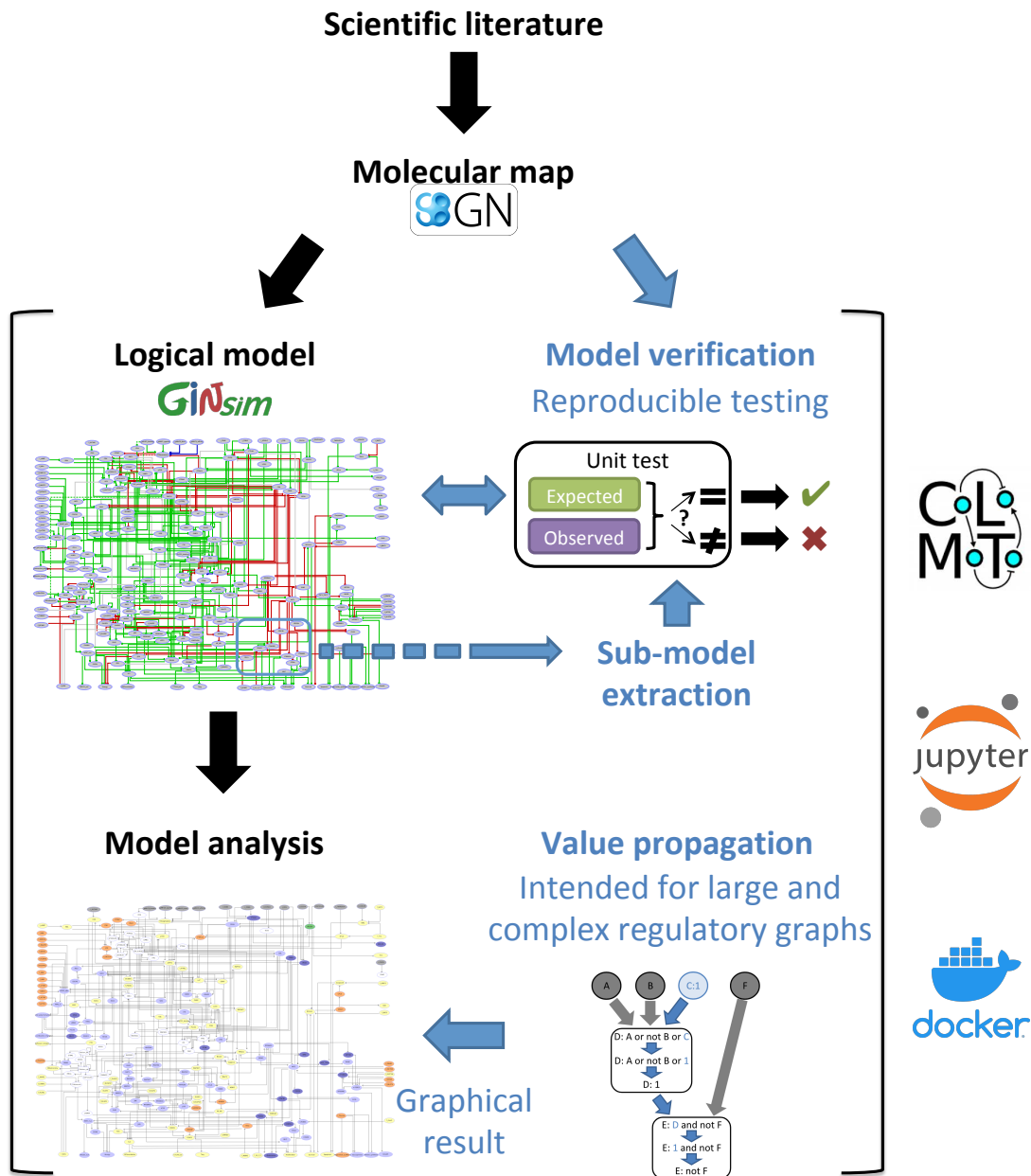


Figure 1. Description of the proposed workflow for the development and analysis of dynamical logical models. The novel methods described in this article are emphasized with blue fonts. Starting with the delineation of a molecular map integrating the available scientific knowledge, we derive a regulatory graph and logical rules to generate a logical model, and induce dynamical specifications serving as test cases to verify the model. Moreover, when the available knowledge is specific to a smaller part of the regulatory graph, a sub-model is extracted to perform local tests. We further implemented an analysis and visualisation method, called Value propagation, to assess the impact of environmental and genetic perturbations. Figure 3 zooms into this part of the workflow and describes it in more details. The use of model verification, sub-model extraction and value propagation is illustrated in two reproducible and editable Jupyter notebooks, taking advantage of the CoLoMoTo Interactive notebook framework (Naldi et al., 2018b). This framework is available inside the CoLoMoTo Docker image together with packaged libraries for the analysis of dynamical logical models of biological networks.

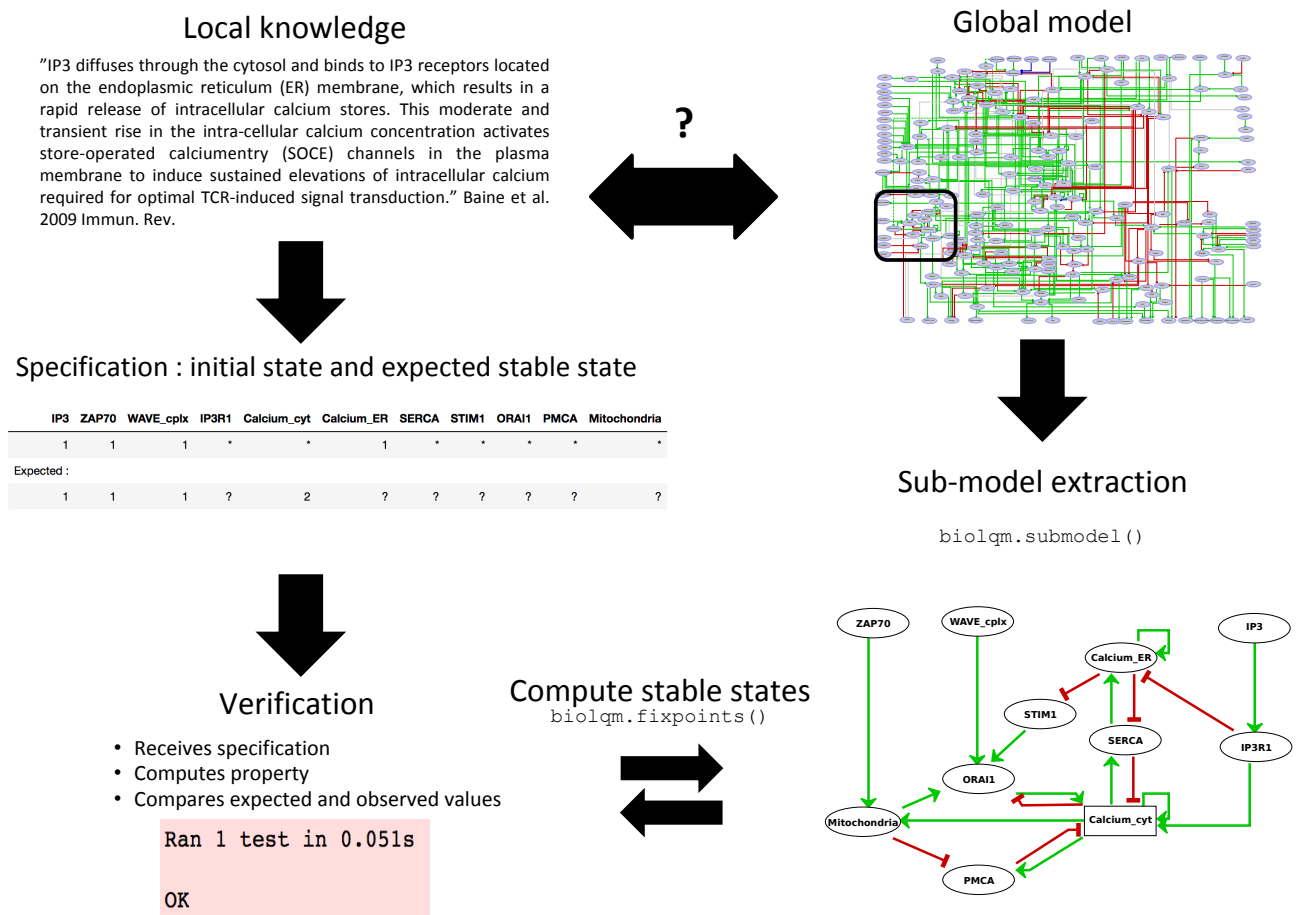


Figure 2. Sub-model extraction for local model verification. When the available knowledge is fragmentary and covers the behaviour of only a subset of components, verification becomes difficult at the global scale of the model. Based on this partial information, a series of specifications can still be defined for a sub-model which, after extraction using bioLQM’s `submodel()` function, can then be rigorously tested.

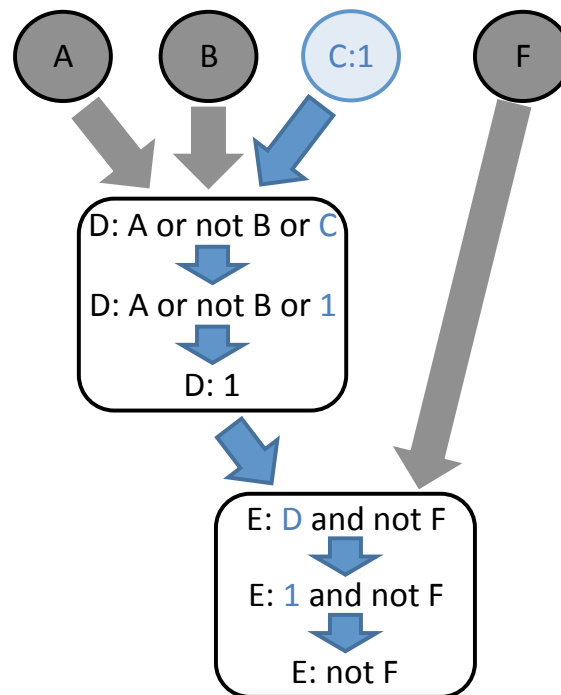


Figure 3. The principle of logical value propagation analysis is illustrated with a simple example involving two core nodes, D and E, and four input nodes, A, B, C and F. The value 1 is assigned to the node C and then propagated through the model. The assignment C:1 implies the evaluation of D to 1. Consequently, the function assigned to node E becomes 'not F'. In other words, assigning the value 1 to node C activates node D independently from the value of its other inputs, while node E becomes completely dependent on the value of node F.

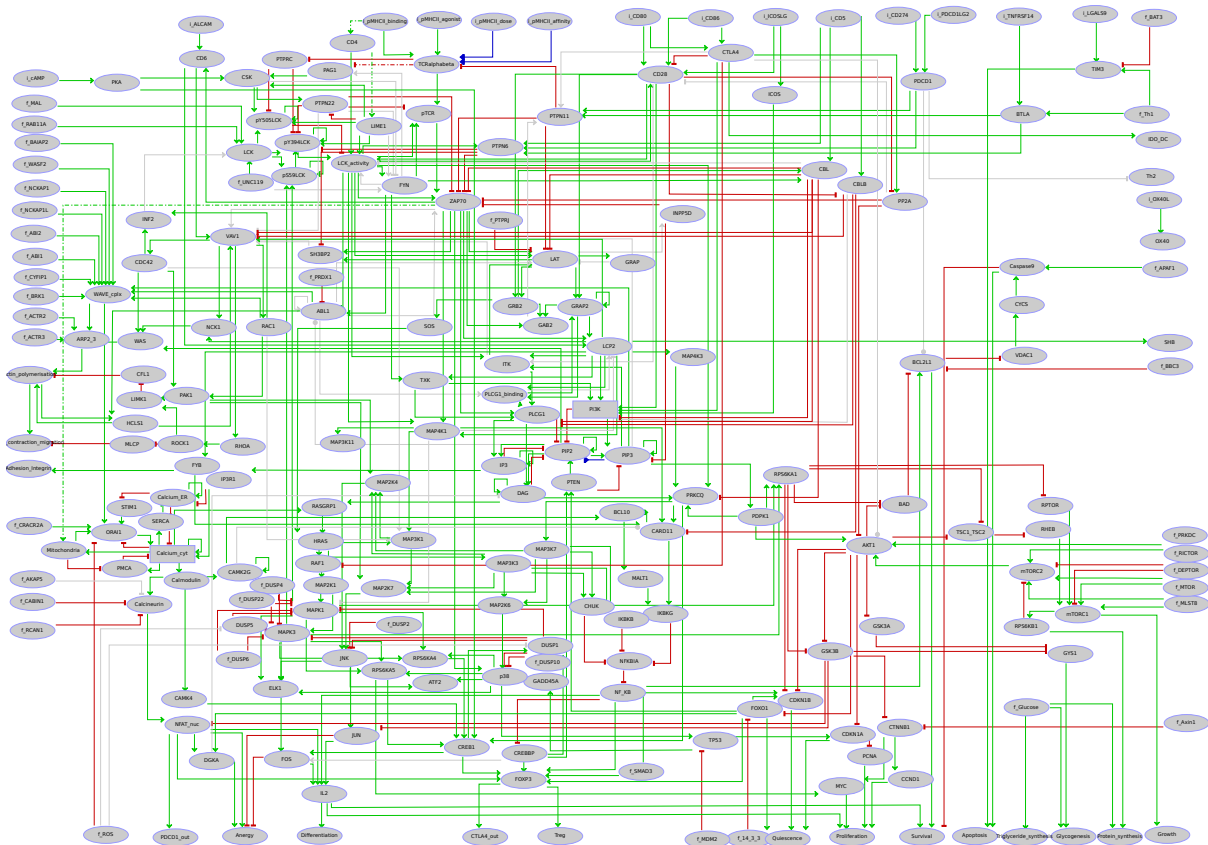


Figure 4. Regulatory graph of the T cell activation model. The global layout is similar to the molecular map (cf. supplementary Figure 1 and supplementary File 1), with ligands/receptors and proximal signalling at the top, and the nucleus-related events at the bottom of the graph. In between, the model encompasses interconnected pathways and signalling cascades related to cytoskeleton remodelling, the MAPK network, calcium fluxes, metabolic shifts, and NF- κ B, to name a few. Boolean components are denoted by ellipsoids whereas rectangles denote ternary components. Green arcs denote activation events, red blunt arcs denotes inhibitions, while blue arcs denote dual regulations. The grey arcs represent interactions created during the translation of the molecular map into the regulatory graph, but that are not yet integrated at the dynamical level (i.e. not taken into account in the logical rule).

Context	Expected behaviour (active or inactive components)
<i>Global specifications</i>	
No stimulation	Active: Quiescence, Glycogenesis
Non-optimal stimulation (antagonist or low/high dosage/affinity)	Active: Anergy (DGKA), Quiescence, Glycogenesis
Optimal stimulation	Active: Differentiation, IL2, Proliferation, Growth, Actin polymerisation, Actin contraction
CTLA4 stimulation	Active: Quiescence
PD-1 stimulation	Active: Quiescence
<i>Local specifications for the calcium module</i>	
Absence of IP3R stimulation, Calcium in ER	Active: Calcium_ER; Inactive: IP3R1
Absence of IP3R stimulation, Calcium in the cytoplasm	Active: Calcium_ER; Inactive: IP3R1
IP3R stimulation, Calcium in ER	Active: IP3R1, Calcineurin; Inactive: Calcium_ER

Table 1. Global specifications used to assess the T cell activation model and example of local specifications for the calcium signaling module (cf Figure 2). After verification, named components should have a value of 0 if specified as inactive, while active components should have a value of 1 or 2. Verification of local specifications requires the extraction of a sub-model from the global model. These verifications and literature references are detailed in the companion CoLoMoTo notebooks. ER: Endoplasmic Reticulum.

Impact of value propagation	CTLA4 ON	PD-1 ON	Intersection
Frozen inactive nodes	105	47	47
Frozen active nodes	28	13	12
Free nodes	29	102	28

Table 2. Quantification of the model nodes impacted by the propagation of CTLA4 or PD-1 persistent activation. After propagation, the nodes of the model can remain free (not fixed) or become frozen inactive (value 0) or frozen active (value 1, or potentially higher in the case of multilevel components). The model encompasses a total of 216 nodes, including 14 inputs and 40 nodes not affected by CTLA4 or PD-1 activation. Interestingly, PD-1 itself is the only single node specifically frozen by its activation (and not by the activation of CTLA4). Furthermore, each of 59 nodes affected by the two perturbations is frozen to the same value in both cases. Details of the computation method can be found in the companion CoLoMoTo notebooks.